

Highly sensitive and selective of two coumarin-based fluorometric probes for detection of ClO^- and cell imaging

Lei Jin,^{1,2} Xiaoxue Tan,¹ Cong Zhao,¹ Qingming Wang,^{1,*}

¹School of Pharmacy, Jiangsu Provincial Key Laboratory of Coastal Wetland Bioresources and Environmental Protection, Yancheng Teachers' University, Yancheng, Jiangsu 224051, People's Republic of China;

²College of Biotechnology and Pharmaceutical Engineering, Nanjing University of Technology, Nanjing, 210009, People's Republic of China.

Corresponding authors. E-mail: wangqm@yctu.edu.cn

Fig.S1. The FI-IR spectrum of **BCO**

Fig.S2. The FI-IR spectrum of **BETC**

Fig.S3. ESI-MS spectrum of **BCO**

Fig.S4. ESI-MS spectrum of **BETC**

Fig.S5. ¹H-NMR spectrum of **BCO**

Fig.S6. ¹³C-NMR spectrum of **BCO**

Fig.S7. ¹H-NMR spectrum of **BETC**

Fig.S8. ¹³C-NMR spectrum of **BETC**

Fig S9. Fluorescent emissions spectra of **BCO** & **BETC** (1.0 μM) in the presence of ClO^- . (A) for **BCO**; (B) for **BETC**.

Fig S10. (a) Fluorescence emission spectrum for **BCO** (1.0 μM) and different metal ions ($\lambda_{\text{ex}} = 372 \text{ nm}$). Inset: The visible fluorescence changes upon Uv irradiation. (b) Fluorescence emission spectrum for **BETC** (1.0 μM) and different metal ions ($\lambda_{\text{ex}} = 350 \text{ nm}$). Inset: The visible fluorescence changes upon Uv irradiation.

Fig S11. ESI mass spectra of **BETC** upon addition of excess ClO^- .

Fig S12. ¹H-NMR spectrum of **NOA**

Fig S13. ¹³C-NMR spectrum of **NOA**

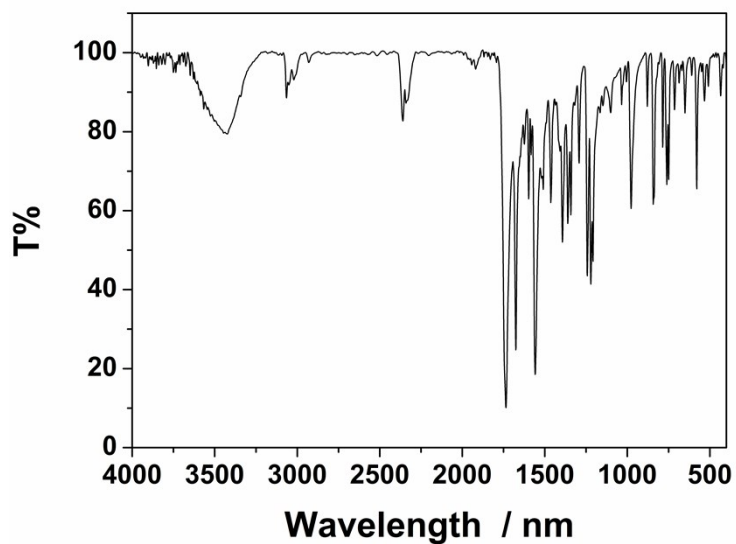


Fig.S1. The FI-IR spectrum of **BCO**

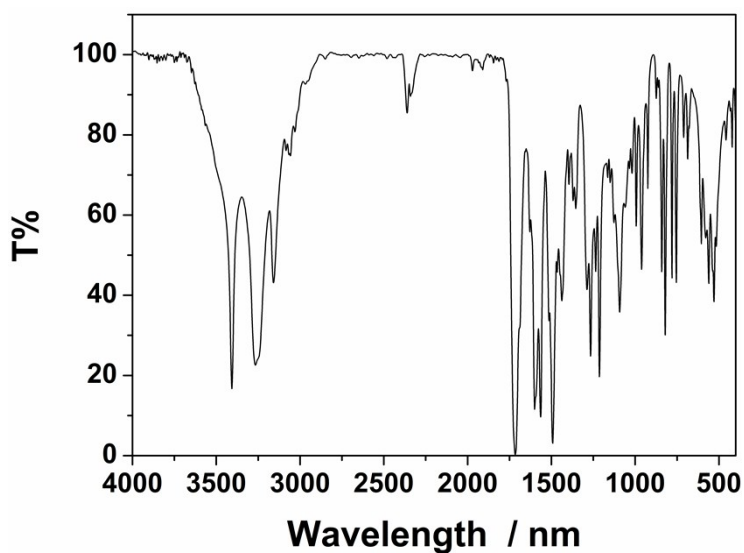


Fig.S2. The FI-IR spectrum of **BETC**

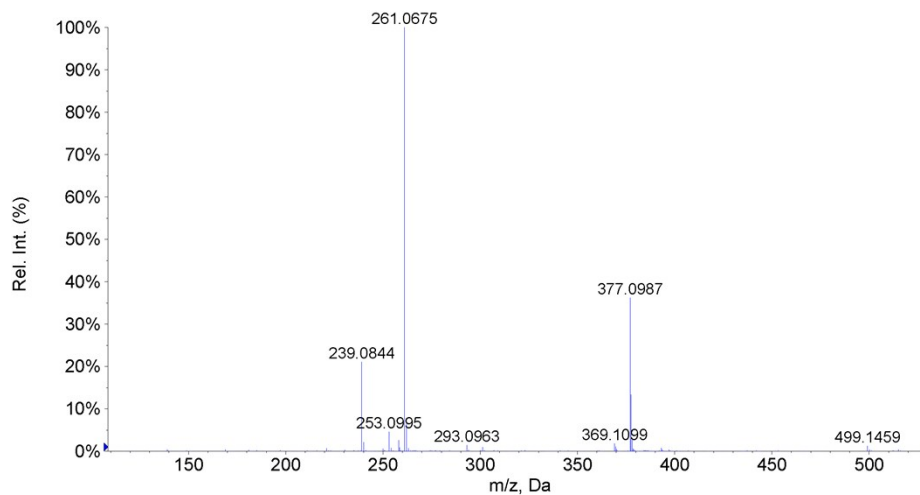


Fig.S3. ESI-MS spectrum of **BCO**

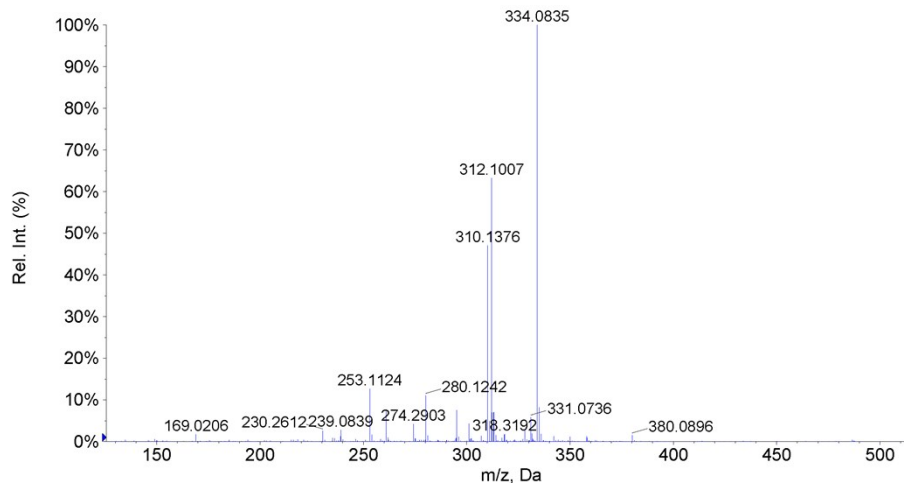


Fig.S4. ESI-MS spectrum of BETC

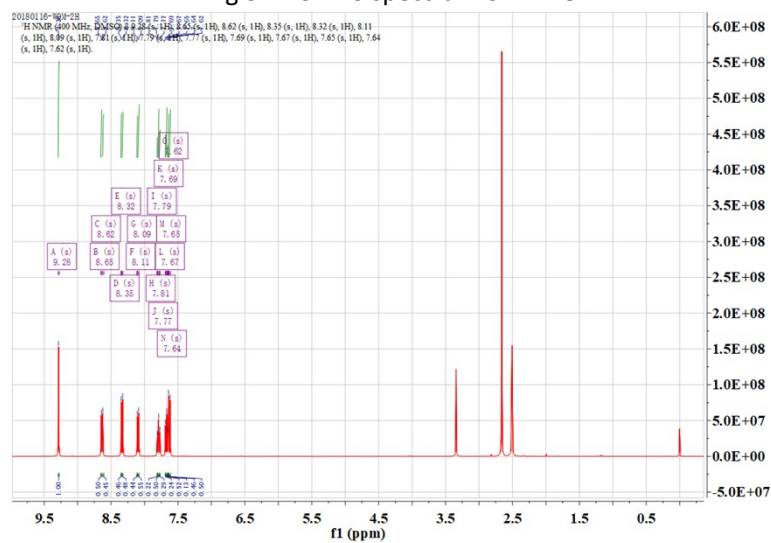


Fig.S5. ¹H-NMR spectrum of BCO

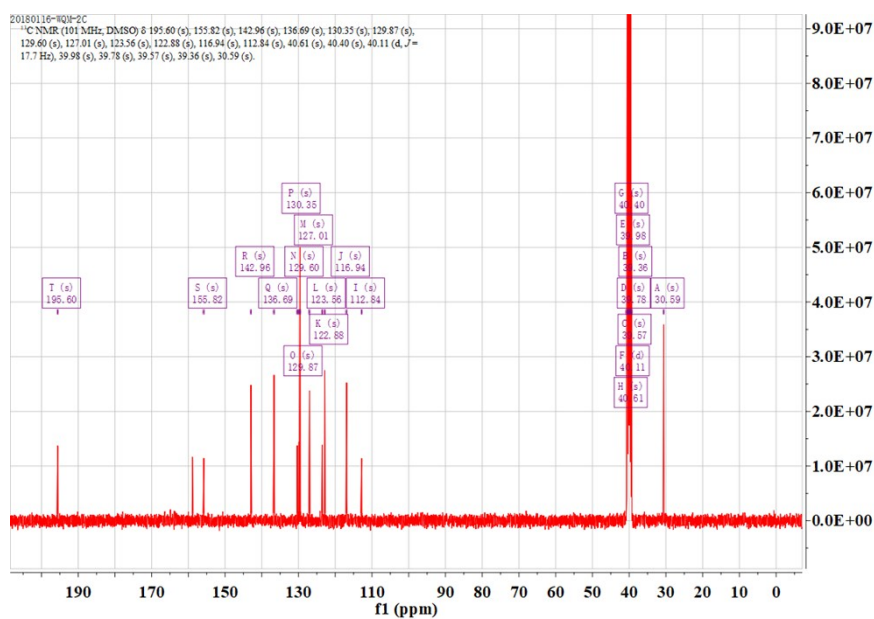


Fig.S6. ¹³C-NMR spectrum of BCO

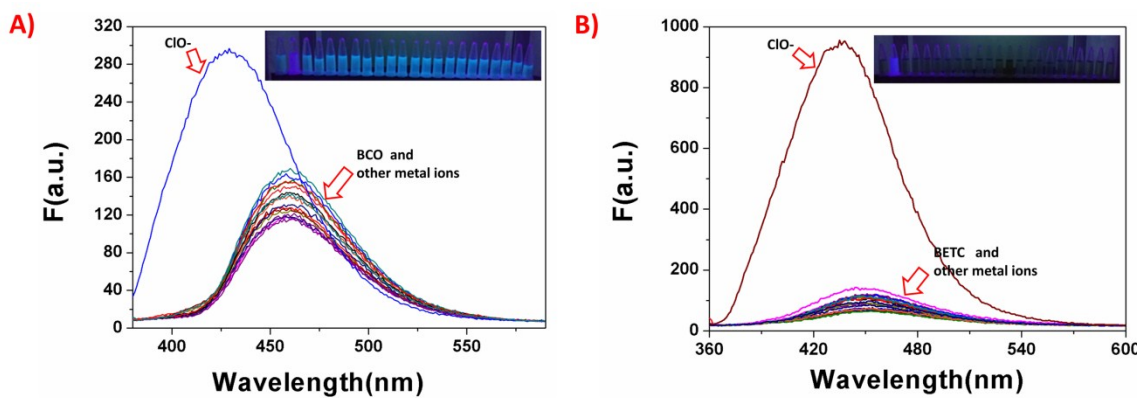


Fig S10. (a) Fluorescence emission spectrum for **BCO** (1.0 μM) and different metal ions ($\lambda_{\text{ex}} = 372 \text{ nm}$). Inset: The visible fluorescence changes upon UV irradiation. (b) Fluorescence emission spectrum for **BETC** (1.0 μM) and different metal ions ($\lambda_{\text{ex}} = 350 \text{ nm}$). Inset: The visible fluorescence changes upon UV irradiation.

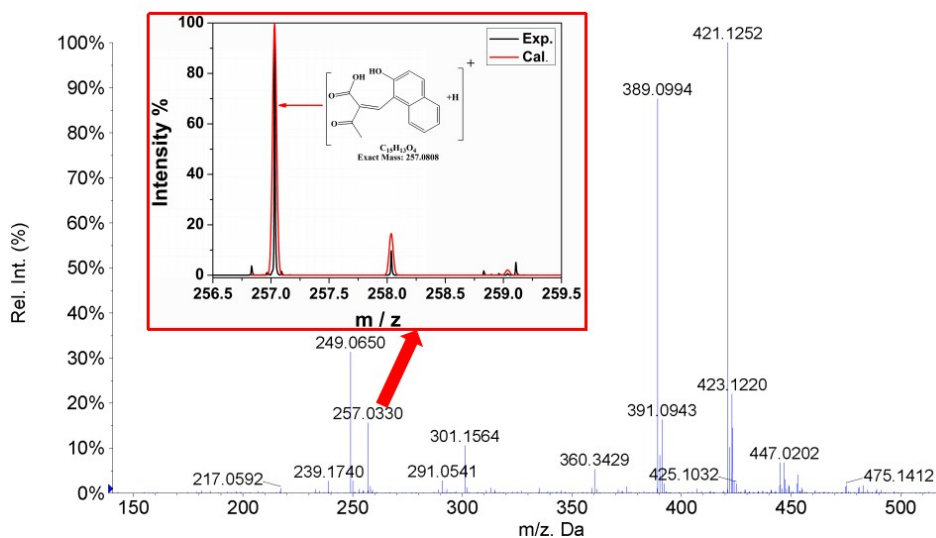


Fig S11. ESI mass spectra of **BETC** upon addition of excess ClO⁻.

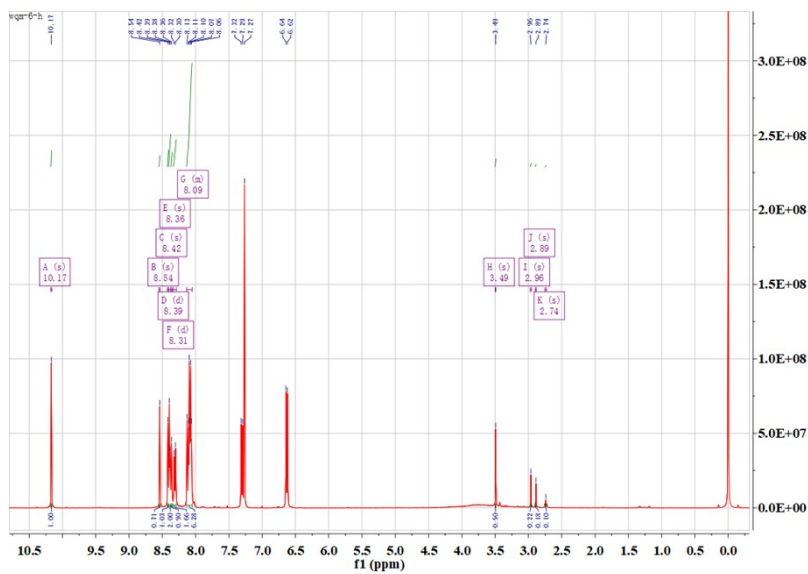


Fig S12. ¹H-NMR spectrum of NOA

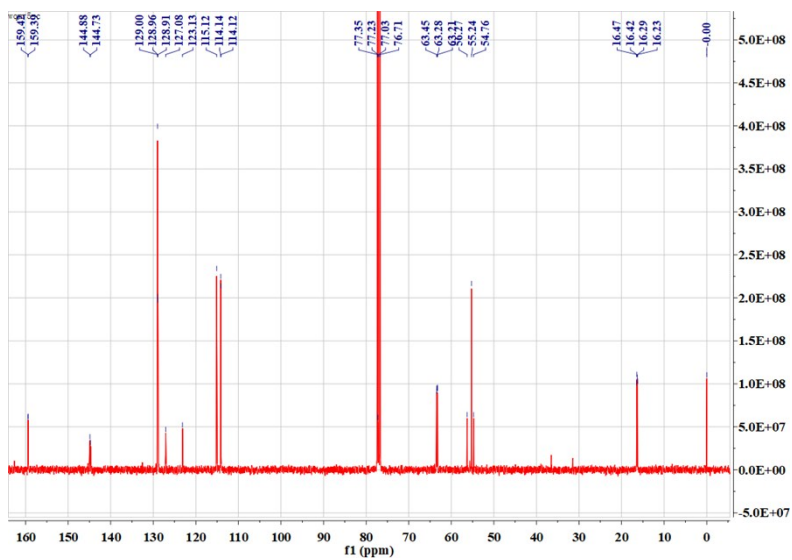


Fig S13. ¹³C-NMR spectrum of NOA

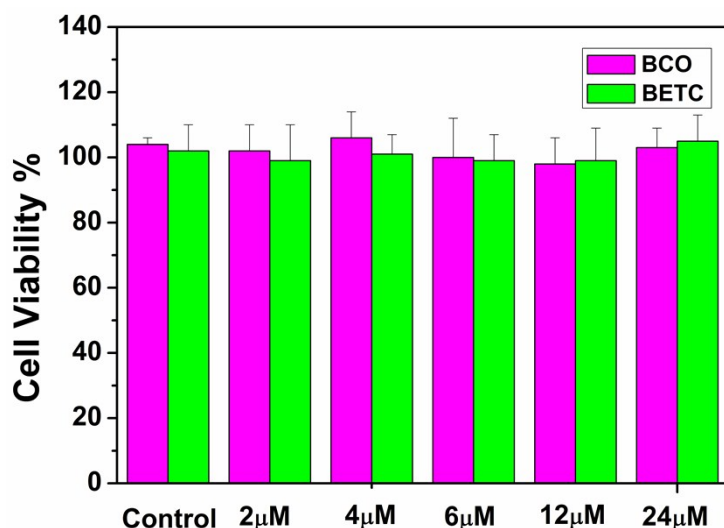


Fig. S14. The cell viability incubated with **BCO** & **BETC** at various concentrations (0, 2, 4, 6, 12 and 24 μM). The experiments were repeated three times and the data were shown as mean value(\pm SD).

Table S1 Compared with other reported methods

LOD / nM	Linear range/ μM	Response Time/S	Application	Reaction media	Reference
5.86	0-40	135	Living cells imaging	Water	[22]
8.2	0-100	1200	Living cells imaging	Water	[23]
—	0.5-5	—	Living cells imaging	Methanol:PBS (5:5,v/v) pH7.4	[25]
0.027	0-0.003	3	Living cells imaging	PBS pH 7.4	[27]
0.43	1-10	30	Living cells imaging	EtOH:PBS (1:9,v/v) pH 7	[30]
—	1-7	60	Living cells imaging	PBS:DMSO (1:9,v/v) pH 7.4	[32]
77.82	0-200.96	16	Living cells imaging	PBS pH 7.4	[36]
182	0-25	120	Living cells imaging	EtOH:PBS (3:7,v/v) pH 7.4	[43]

9.6	0-55	5	Living cells imaging	H ₂ O:CH ₃ CN (4:1,v/v) pH 7.4	[46]
7.0	1-10	60	Living cells imaging	EtOH:PBS (1:9,v/v) pH 7.3	[47]
210	0-18	120	Living cells imaging	EtOH:PBS (1:9,v/v) pH 7.4	[45]
154	0-70		Living cells imaging		This work
32	0-20		Living cells imaging		This work
